

5-2014

# Solid State Synthesis of the SrTiO<sub>3</sub> Nano-particle

Spencer S. Coonrod  
*University of Arkansas, Fayetteville*

Follow this and additional works at: <http://scholarworks.uark.edu/meeguht>

---

## Recommended Citation

Coonrod, Spencer S., "Solid State Synthesis of the SrTiO<sub>3</sub> Nano-particle" (2014). *Mechanical Engineering Undergraduate Honors Theses*. 39.  
<http://scholarworks.uark.edu/meeguht/39>

This Thesis is brought to you for free and open access by the Mechanical Engineering at ScholarWorks@UARK. It has been accepted for inclusion in Mechanical Engineering Undergraduate Honors Theses by an authorized administrator of ScholarWorks@UARK. For more information, please contact [scholar@uark.edu](mailto:scholar@uark.edu).

Solid State Synthesis of The SrTiO<sub>3</sub> Nano-particle

An Undergraduate Honors College Thesis

in the

Department of Mechanical Engineering  
College of Engineering  
University of Arkansas  
Fayetteville, AR

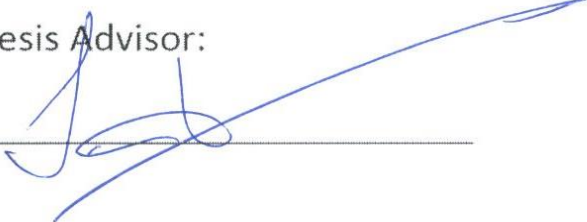
by

Spencer Stayton Coonrod



This thesis is approved.

Thesis Advisor:



---

Thesis Committee:



---



---

## **Abstract**

Recent studies have shown the ability to synthesize perovskite materials through solid state chemical reaction. In previous work at the University Annamalai Naga, a specific perovskite  $\text{SrTiO}_3$  (STO) was created through solid state reaction between strontium carbonate and, titanium dioxide powders that were homogenously mixed and then sintered until completion of the reaction. The sintered powder was characterized by X-ray diffraction (XRD) and shown to be a perovskite structure without evidence of additional phases.

This work specifically reports on the reproducible solid state reaction procedure developed at the University of Arkansas for the production of STO powder, characterization of formed compounds. The phase transformation was confirmed by X-ray diffraction (XRD) analysis and Dispersive X-ray Spectrometry (EDX). Using the procedure 99.9% pure STO powder was produced, with the compound synthesized having similar cubic structure to STO references. EDX characterization agreed with XRD results and showed the formation of a fine powder necessary for pulsed laser deposition (PLD) targets.

Future work can be done in research of the solid state synthesis of more materials from the perovskite group and in optimization and creation of inexpensive pulse laser deposition targets.

Honors Paper/Thesis Duplication Release

[Note: to comply with Public Law 94-553-October 19, 1976 of the 94<sup>th</sup> Congress, and Act for the General revision of the Copyright Law, Title 17 or the United States Code, the following is to be included the paper and signed by the student.]

Honors Paper Duplication and Distribution Release

I hereby authorize the University of Arkansas Libraries to duplicate and distribute this honors paper in any format (including electronic based distribution) when needed for research and/or scholarship.

Agreed (Signature and date): \_\_\_\_\_

Name Typed or Printed: \_\_\_\_\_

## **Acknowledgements**

I would like to thank the faculty and staff of the University of Arkansas Mechanical Engineering and Physics Departments who were directly and indirectly involved with the project. I would especially like to thank Dr. Jak Chakhalian my primary research advisor for his mentorship and direction. I would like to thank Xiaoran Liu for his help with implementation of procedure and his with XRD and EDX characterization at the University of Arkansas. I also thank Dr. Mike Hawkridge and Dr. Mourad Benamara for their help and explanation of the XRD and SEM machines at use in the University of Arkansas. A special thanks to my research advisors in Mechanical Engineering and Physics (Dr. Min Zou and Dr. Gay Stewart, respectively) and all of the graduate students I have had the chance to work with over the past year.

## Table of Contents

Abstract .....	1
Acknowledgements.....	3
1. Introduction .....	6
2. Experimental .....	8
3.1 Characterization Methods.....	14
3.1 X-Ray Diffraction .....	14
3.2 Scanning Electron Microscopy .....	16
3.3 Dispersive X-ray Spectrometry.....	14
3.4 Reference Data .....	18
4. Characterization and Results .....	21
4.1 X-Ray Diffraction Sample 1 Results .....	22
4.2 X-Ray Diffraction Sample 2 Results .....	25
4.3 X-Ray Diffraction Sample 3 Results .....	28
4.4 Dispersive X-ray Spectrometry Sample 2 Results .....	31
4.5 Dispersive X-ray Spectrometry Sample 2 Results .....	34



5. Conclusions .....	37
6. Future Work .....	38
Works Cited .....	39
Appendices.....	40
A1 Oven Setup.....	40
B1 Data Peak List.....	42

# 1. Introduction

Thin Films and Nano-materials in recent years have been producing momentous research interests due to their fundamental significance for addressing some rudimentary issues in fundamental physics, as well as their potential applications as advanced materials.[1] Strontium titanate,  $\text{SrTiO}_3$  (STO), an  $\text{ABO}_3$  perovskite, is debatably the prototypical member of this structure family, not only because it can be made to exhibit a diverse range of unusual properties itself.[2] Moreover, STO is an important band insulator (energy gap = 3.2 eV) and is becoming the basis for the emerging field of oxide electronics in condensed-matter research. STO has been heavily researched for its unique physical properties, such as its good insulation, and many practical applications, such as photo-catalysts in solar cells, and solid oxide electronic devices.[1]

In past years the University of Arkansas would acquire  $\text{SrTiO}_3$  nano-particles from commercial sources, in order to obtain 99.9% pure particles with the correct shape and specification for use in experimentation, specifically especially in the areas of thin film fabrication using the Pulsed Laser Deposition (PLD) technique.. STO is commonly used as a sputtering target in the PLD process in or to create epitaxial growth on a substrate. Recently laboratory methods have been published for solid state synthesis of STO with purity and characteristics equivalent to that of commercial grade nano-particles available now.

The work of this thesis will be focused on creating a reproducible procedure for laboratory creation of STO nano-particles equivalent to those of commercial quality. Validating this procedure will be done by characterizing the created particles and comparing these properties to cataloged properties. Characterization will be carried out primarily by powder X-ray diffraction (XRPD) and Dispersive X-ray Spectrometry (EDX).

## 1.1 Pulse Laser Deposition

Pulsed Laser Deposition (PLD) is a subcategory of an epitaxial growth method called Physical Vapor Deposition (PVD). Epitaxial growth involves growing films atomic layer by atomic layer on a substrate. One of the most common methods for epitaxial growth is physical vapor deposition. The process of vapor deposition is a process where a “solid immersed in a vapor becomes larger due to material deposited from the vapor onto the solid surface”. [3] The solid the materials deposited on will be called the substrate. In this case the material to be deposited is vaporized by physical means (a laser pulse).

Pulsed laser deposition is a physical vapor deposition process, carried out in a vacuum system; pulsed lasers are focused onto a target of the material to be deposited.

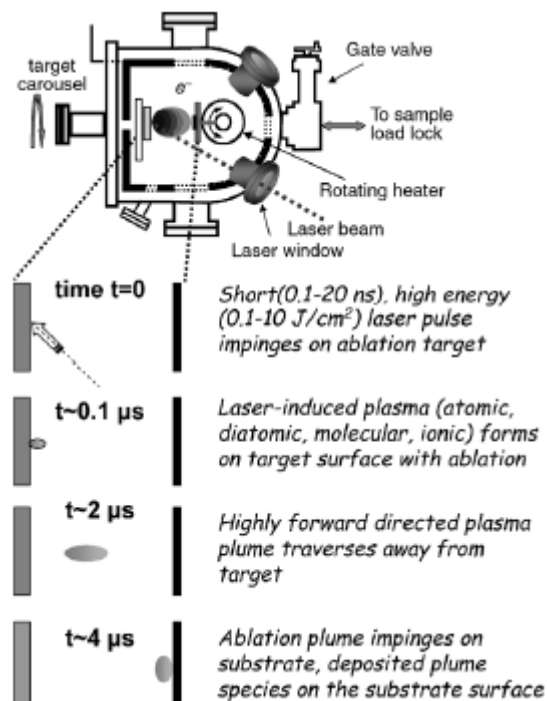


Figure 1.1:PLD Diagram [4]

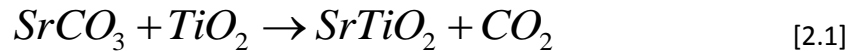
Figure 1.1 shows a plasma vapor deposition with a high laser energy density, each laser pulse vaporizes a small amount of the material creating a plasma plume. The vaporized material is expelled from the target in a forward-directed vapor plume. [4]

One of the most significant characteristics of PLD is the ability to transfer material with precise stoichiometric quantities. This is due to absorption of the high laser energy pulse by a small volume of material, instead of a process which heats the entire material to cause vaporization. For other PVD methods would simply heat the target, with the ejected vapor due to thermal evaporation of the target. [4]

## 2. Experimental Methods

The STO sputtering target powders were made through solid reactions between Strontium Carbonate and Titanium Oxide powder. All the powders had 99.9% purity and were mixed in agate mortar using isopropyl alcohol up to dryness. Mixed powder was sintered then milled again to destroy agglomerates. The sintered powder was characterized by XRD and showed a perovskite structure without evidence of additional phases. [2]

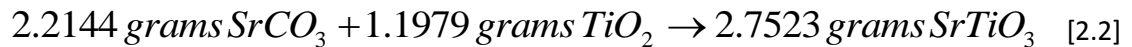
The Stoichiometric ratios and reaction equation are shown below in **Equations 2.1 and 2.2.**



$$SrCO_3 = 147.628 \text{ grams per mole}$$

$$TiO_2 = 79.865 \text{ grams per mole}$$

$$SrTiO_3 = 183.484 \text{ grams per mole}$$



The formula shows a 1-to-1 molar ratio needed between the two chemicals to produce SrTiO<sub>3</sub>.

One mole of SrCO<sub>3</sub> was found to be 147.628 grams and one mole of TiO<sub>3</sub> was found to be 79.865 grams. To produce approximately 2.7 grams of SrTiO<sub>2</sub>, 0.015 moles of each chemical were added to the mixture. The catalyst in this chemical reaction was the heat supplied from the oven.

Chemical powders were measured in a 0.015 molar ratio in order to produce approximately 2.7 grams of SrTiO<sub>3</sub> powder from the solid state reaction. The process of measuring consisted of calibrating an electronic scale, placing a 4-by-4 inch weighing paper on the scale and then zeroing the scale. After this, experimenters used a disposable laboratory spatula to add powder to the scale. This is shown below in **Figure 2.1**.

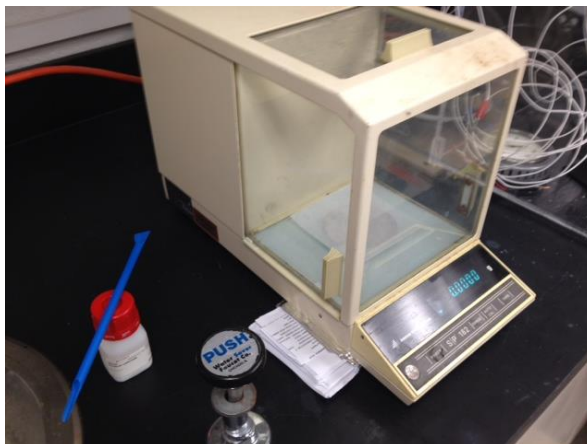


**Figure 2.1: Scale**

Powders were measured out to an accuracy of four decimal place or .0001 grams. First the SrCO<sub>3</sub> was measured out onto the weighing paper, the paper and its powder contents were removed after the weighing and the powder was added to the grinding mortise. This is shown in **Figures 2.2 and 2.3** below.



**Figure 2.2: Weight Measure**



**Figure 2.3: Mortise**

The mortise was then covered with aluminum foil to prevent contamination (in Figure 2.4).



**Figure 2.4: Covered Mortise**

The  $\text{TiO}_2$  powder was then measured out and added to the mortise using the same methodology and accuracy as the previous powder (Measured weight shown in **Figure 2.5**).

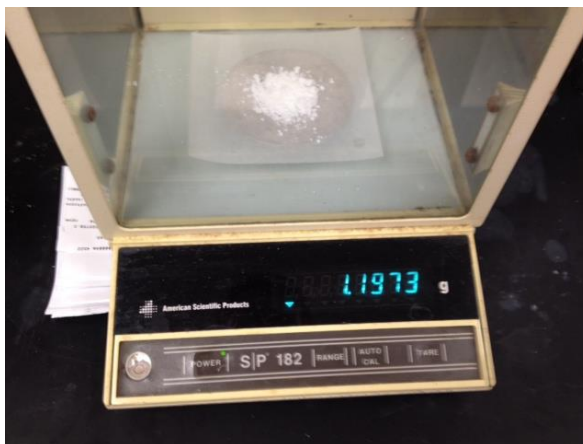


**Figure 2.5: Weight Measure**

The powder was then homogeneously mixed by applying one fluid ounce of laboratory grade isopropyl alcohol to the mixture and then grinding until the alcohol was completely evaporated (Shown below in **Figure 2.6**).



Once evaporation is completed the now homogeneous powder is scraped into the center of the mortar and then ground evenly for approximately 3 hours by hand, switching from clockwise to counterclockwise every 30 minutes (illustrated in **Figure 2.7** below).



**Figure 2.7: Grinding**

After the grinding, the powder was moved to a ceramic container to be heated inside of the oven (**Figure 2.8**).



**Figure 2.8: Ceramic Containers**

After the sample was placed in the oven it was heated using the ovens step heat program. Details of the program can be found in **Appendix 1.3**. The relevant information is that the sample was heated incrementally and held at 600 degrees Celsius for 15 minutes to account for the heat required to warm the ceramic container. Various heating temperatures and times were tested to achieve the desired outcome. These samples are shown in **Table 2.1**.



**Table 2.1: Heating Procedures**

<b>Maximum Temperature</b>	<b>Time Held at Maximum Temperature</b>
<b>800 C</b>	<b>8 hours</b>
<b>1300 C</b>	<b>12 hours</b>
<b>1000 C</b>	<b>10 hours</b>

### 3. Characterization Methods

Target powders were primarily analyzed by X-ray powder diffraction (XRPD) and energy dispersive X-ray spectrometry (EDX) a form of scanning electron microscopy (SEM).

#### 3.1 X-Ray Diffraction

Diffraction occurs when an X-ray excites an electron which emits an electromagnetic field at the same frequency. Atoms in the same structure emit a wave from the excitation from the first atom this creates an interference pattern. X-rays are employed in characterization methods because the wave length of an X-ray is on the order of a few angstroms.[5] This length is relatively close to the distance between atoms in most crystalline solids, making the X-ray able to produce distinct interference patterns as a result of diffraction.[5] Constructive interference occurs when two waves are moving in phase amplifying each other. Destructive interference occurs when two waves are out of phase by 180 degrees and cancel each other out. This can be seen in **Figure 3.1**.

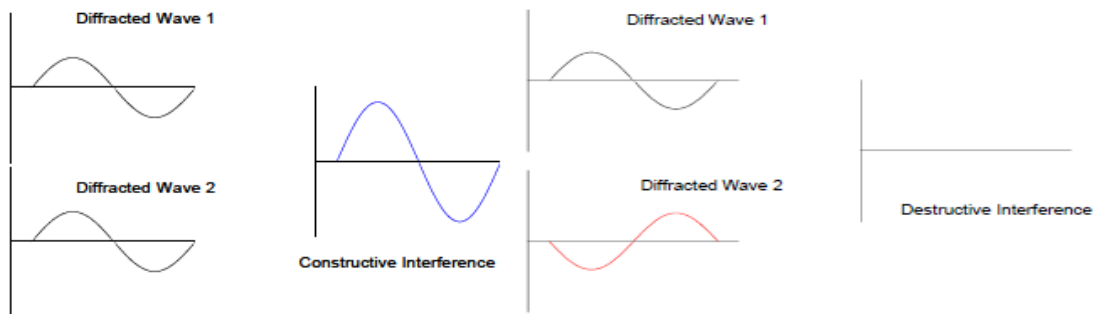


**Figure 3.1**

XRPD is used for phase identification and phase compositions. When performing XRD, a machine produces a beam of X-rays which strikes the powder and is diffracted. The X-rays are then scattered at various angles and resulting intensities, then the rays are collected by a detector.[5] Incident X-ray's will come into contact with atoms at different points in the lattice structure of a

material creating constructive and destructive wave fronts which produce diffracted X-ray peaks varying in location and intensity, this is shown in **Figure 3.2**.

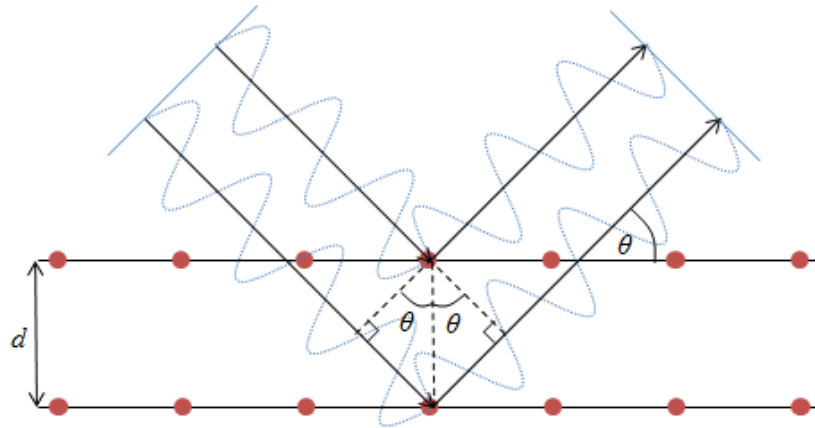


**Figure 3.2**

Because the samples are in powder form, incident X-rays come into contact with the sample in every possible axial orientation. The effect produces a diffraction pattern of cones varying in location and intensity. This allows the detector to complete one linear orbit and collect all diffraction peaks and intensities. Every crystalline substance will give a distinct diffraction pattern or spectra, the composition of a powder and quantities of each substance can be determined based on the XRPD graph's peaks of intensity and corresponding angles. A sample diffraction pattern is shown below in **Figure 3.3**.

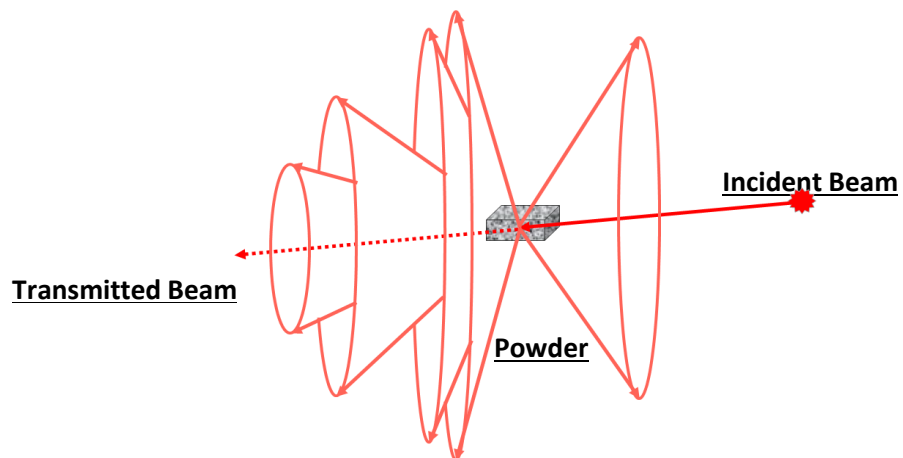


**Figure 3.3: XRPD Diffraction Pattern**

The experimental diffraction patterns can be recorded and can be matched to known prerecorded diffraction patterns (See Figure 4.1 in Section 4 for an illustration of an X-ray diffraction pattern).

### 3.2 Scanning Electron Microscopy

A SEM microscope focus beams of high energy electrons on to a sample, such as a surface of a solid. The interaction from this electron bombardment can then be recorded to determine the samples physical shape, texture, crystalline structure, and even chemical composition. [6] The setup of a typical SEM is shown in the figure below:

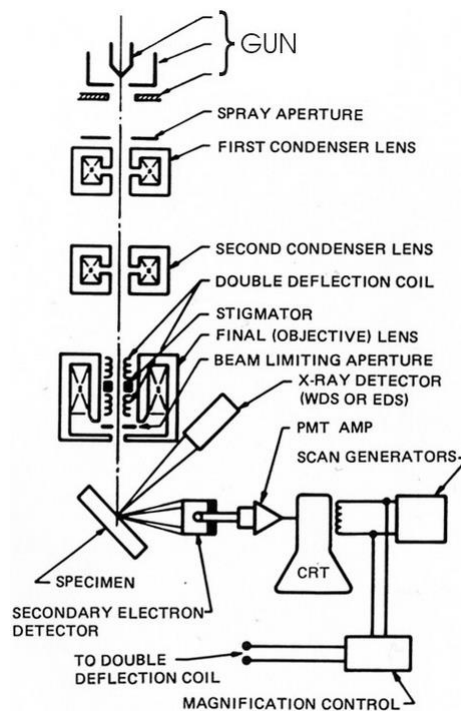


Figure 3.4: SEM Microscope Diagram [6]

The SEM has four basic components. First the electron source shown as “GUN” in **Figure 3.4** is the source of the high energy electrons. Typically tungsten is heated by a high voltage that passes through it expelling electrons. The electrons are then expelled into the second component the magnetic lenses, labeled in **Figure 3.4** by “Condensers” and “Aperture”. These lenses focus the electron beams with a magnetic force and alter the trajectory of the beam in

the scanning process. The third component, not labeled in the figure, is a high vacuum chamber. The chamber prevents electrons from interacting with other particles before reaching the sample. The fourth component is the electron detector. In this case it is the assembly starting with the “secondary electron detector” in **Figure 3.4**. This component attracts and collects “secondary electrons” and “back-scattered electrons” which are lower energy electrons resulting from a collision with the sample. The collector voltage can be adjusted to target certain groups of scattered electrons. The corresponding brightness of a scanned area is then directly related to the number of scattered electrons collected. [6]

This method produces two-dimensional scans of the surface of the sample. SEM is considered to be non-destructive; meaning it does not cause volume loss of the sample. So it is possible to scan the same sample repeatedly. A convenient side effect of the electron bombardment is the emission of X-rays when excited electrons return to lower energy states. These X-rays can be used to determine the elemental composition of the sample. [6] As mentioned earlier, energy dispersive X-ray spectrometry is a specific subset of SEM, discussed in the next section.

### **3.3 Dispersive X-ray Spectrometry**

This method takes advantage of the X-ray spectrum emitted by the atoms of a solid when bombarded by a focused beam of electrons such as in SEM. Analysis of EDX is similar to that of XDR in that a Fourier spectrum of the diffracted sample is compared to known spectra of elements already found experimentally. Being a subset of SEM, the EDX employs a scanning method to produce a surface topography or element mapping. [7]

It is important to state that this diffraction identification method can obtain accuracy greater than  $\pm 1\%$ . Analytical accuracy is commonly nearer  $\pm 2\%$ . The EDX method can be used for elements whose atomic numbers range from 4 to 92 (or from Be to U). [7]

### 3.4 Referenced Data

The reference data used to analyze samples is shown in this section. Strontium Titanium Oxide, Strontium Carbonate, and Titanium Oxide were the primary contributors therefore the discussion will be limited to those compounds. Strontium Titanium Oxide (STO) is an inorganic ceramic mineral whose chemical formula is  $\text{SrTiO}_3$ . The reference data for STO as well as the reference data for all references used in XRPD characterization was from samples done by National Lead Company. The mineral name of the compound is Tausonite. STO's XRPD reference pattern is shown below in **Figure 3.5**. The specific peak list can be found in **Appendix B1**.

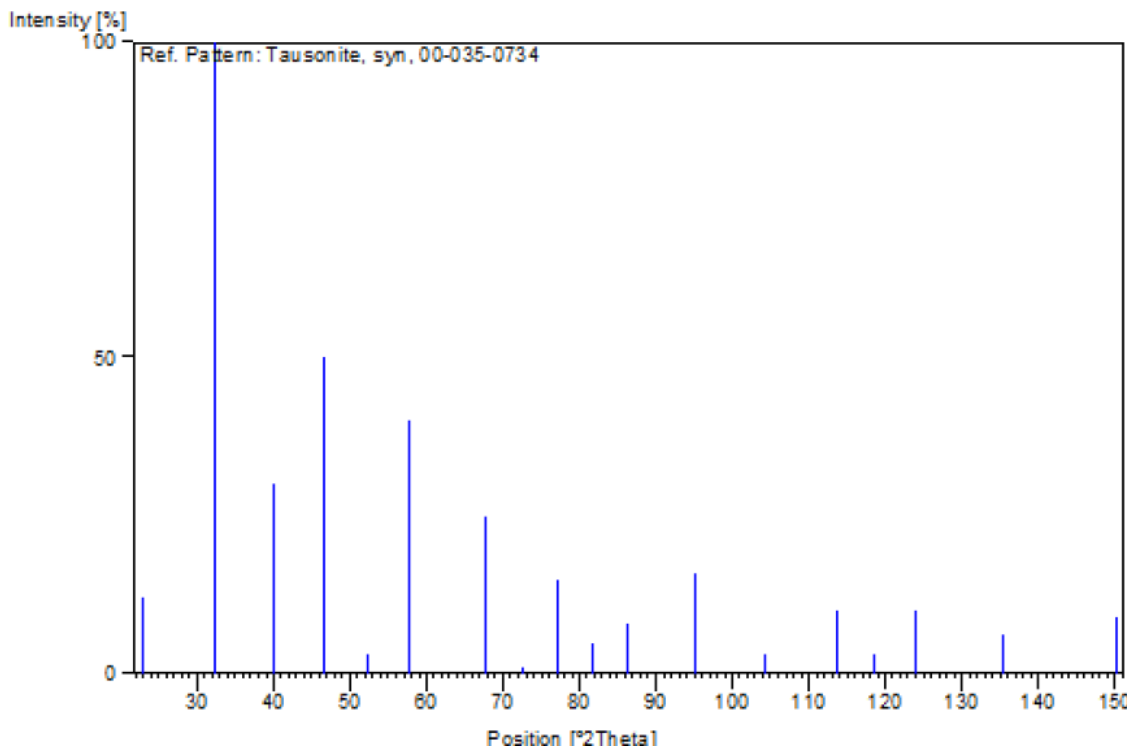


**Figure 3.5: STO Reference Diffraction Pattern**

Titanium Oxide is an inorganic alloy mineral whose chemical formula is  $\text{TiO}_2$ . The reference data for Titanium Oxide used in XRPD characterization was from samples done by National Lead Company. The mineral name of the compound is Rutile. Titanium Oxide's XRPD reference pattern is shown below in **Figure 3.6**. The specific peak list can be found in **Appendix B1**.

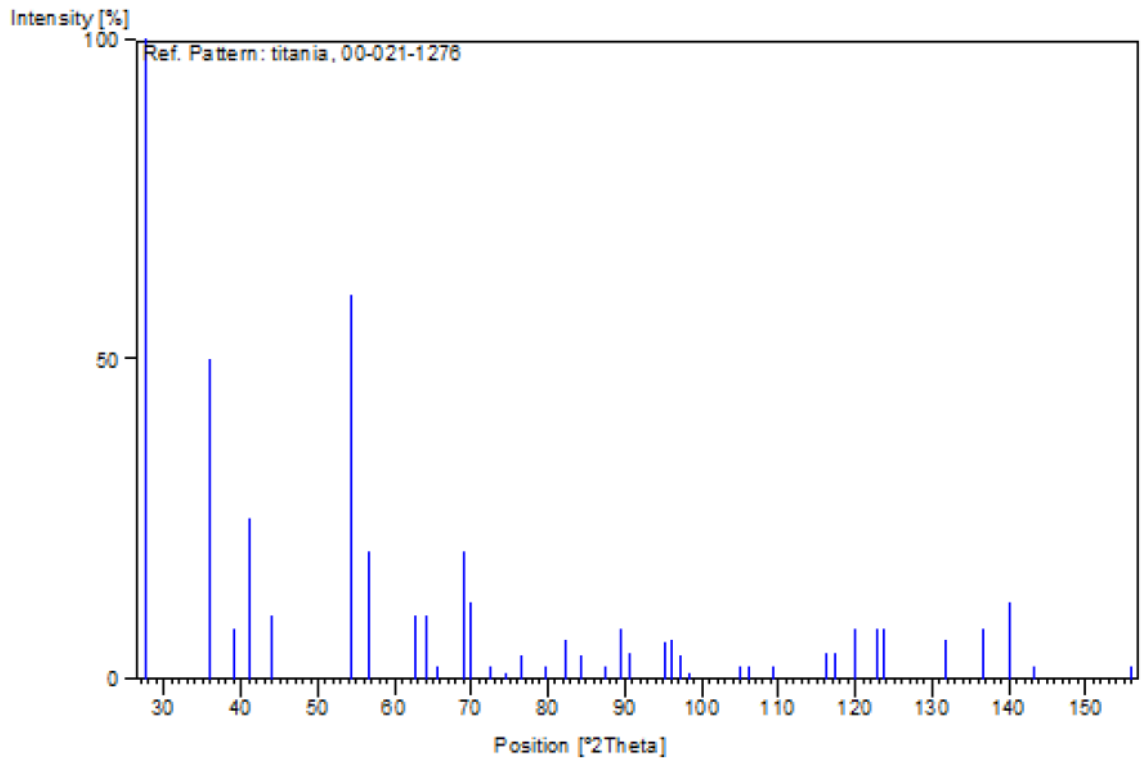


**Figure 3.6:  $\text{TiO}_2$  Reference Diffraction Pattern**

Strontium Carbonate is an inorganic mineral whose chemical formula is  $\text{SrCO}_3$ . The reference data for Strontium Carbonate used in XRPD characterization was from samples done by National Lead Company. The mineral name of the compound is Strontianite. Strontium Carbonate's XRPD reference pattern is shown below in **Figure 3.7**. The specific peak list can be found in **Appendix B1**.

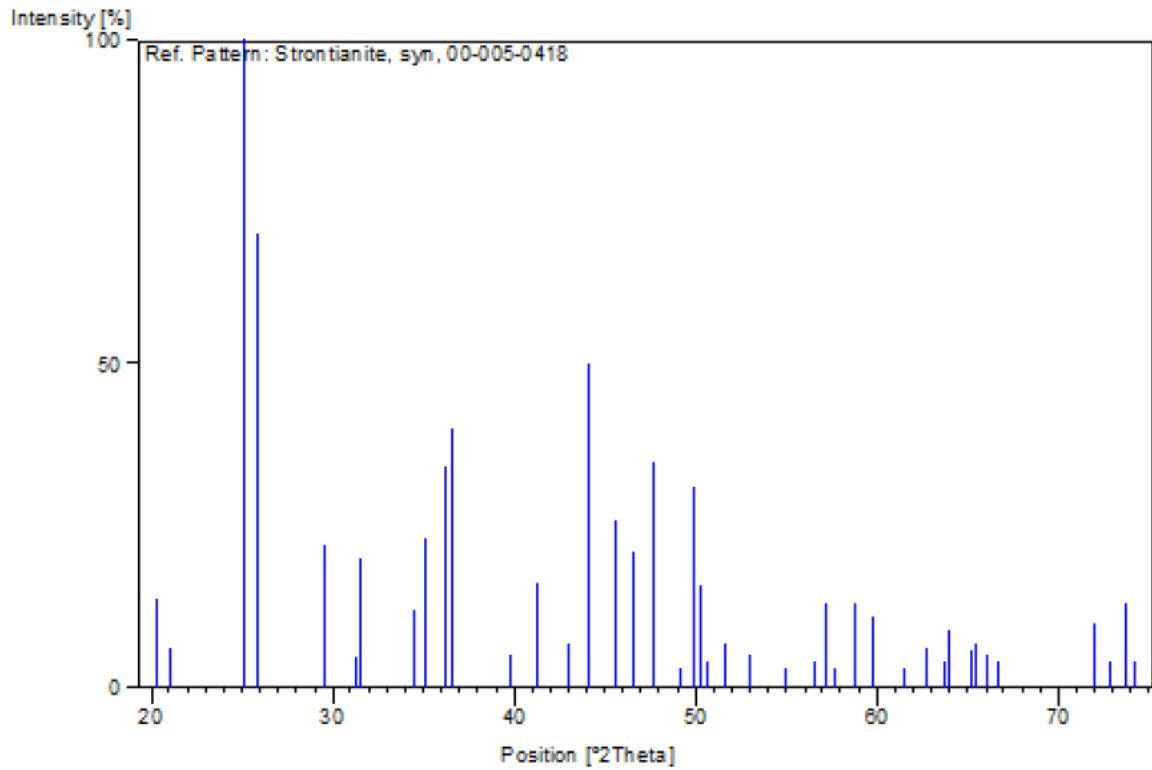


**Figure 3.7:  $\text{SrCO}_3$  Reference Diffraction Pattern**



## 4. Characterization Results

Powder X-ray diffraction was performed at the University of Arkansas, using a Philips PW 1830 X'pert (dual-goniometer X-ray diffractometer). During a single  $\theta$  XRD scan, the x-ray beam emitter is held stationary and the detector is in motion around the sample, which in this case is the powder. The scan occurred within the  $\theta$  range from 20 to 90 degrees with an initial scan time of five minutes and then long scan for thirty minutes.

The X'pert software we use gives a "score" out of 100 that indicates how well the reference pattern from a database fits with the measured data. There are many variables that go into this score algorithm and it can vary depending on the regime that you use, but principally it uses the position and intensity of the most intense peak in the reference as compared to the sample, then the next most intense peak and so on. It is important to know that the X'pert score is not associated with a percent value or total composition ratio.

To find a material composition of a sample the X'pert software uses the Reference Intensity Ratio (RIR), a value associated with each reference, in conjunction with XRD data. The RIR compares peak intensities of the sample to that of the reference. This data with the X'pert software was used to quantify phases, otherwise without the RIR, the program can only identify the phases present.

## 4.1 Sample 1 XRD Results

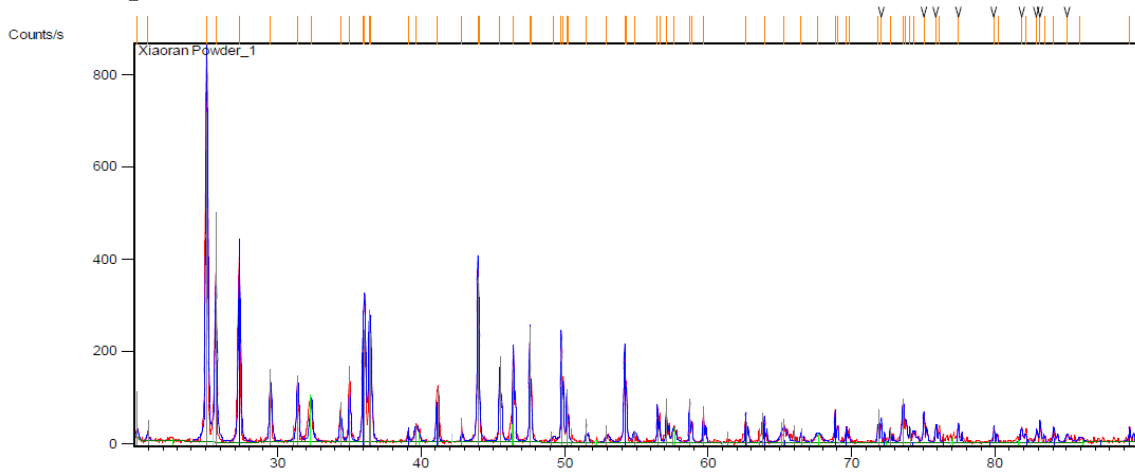


Figure 4.1: Sample 1 Diffraction Pattern

Figure 4.1 above is the spectral graph of the sample which was heated for eight hours at eight hundred degrees Celsius. The y-axis represents the incident X-rays to the detector per second and the X-axis represents the angle  $\theta$  as the scanner travels around the sample. This graph gives the location and intensity peaks of the diffracted X-rays, which we can use to visually compare the sample to the reference data. Figure 4.2 shows many small peaks and broader peak areas, this most likely means that interference from the diffraction pattern of several compounds is being represented. The black V's in the top corner of the figure represent unidentified peaks. These peaks went unidentified because the reference data available for most samples ends after seventy degrees on the spectrum.

### Peak List

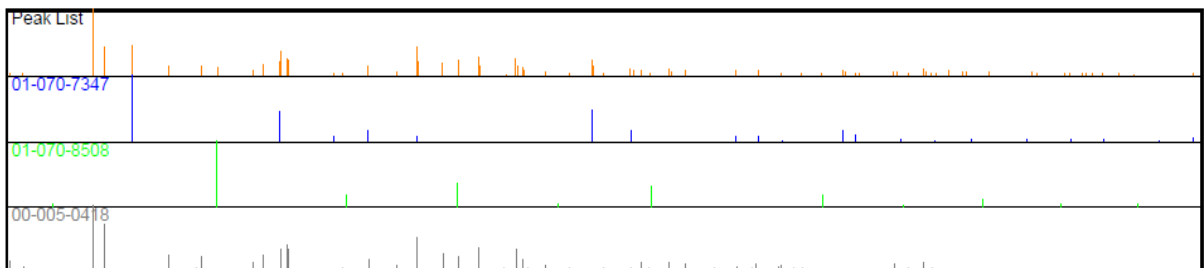


Figure 4.2: Sample 1 Peak List

#### Pattern List

Ref.Code	Compound Name	Chem. Formula	Score	Scale Fac.
01-070-7347	Rutile	Ti O2	57	0.507
01-070-8508	strontium titanate	Sr ( Ti O3 )	34	0.117
01-071-2393	Strontianite	Sr C O3	43	0.873

#### Candidate List

Ref.Code	Compound Name	Chem. Formula	Score	Scale Fac.
00-005-0418	Strontianite, syn	Sr C O3	24	0.603
01-079-1469	Diamond 4H	C	14	0.021
00-050-1082	Carbon	C	14	0.021
00-015-0306	Strontium	Sr	12	0.116
03-065-5959	̂-Sr	Sr	12	0.052

**Figure 4.3: Sample 1 Pattern and Candidate List**

**Figure 4.3** above shows the peak spectrum of first the sample and then the reference spectra that were chosen to compare against it. Diffraction patterns are labeled by their reference code which can be found in the pattern list. The pattern list showed which compounds were selected by the user to compare to the samples diffraction pattern. References in the pattern list were selected from the candidate list based on highest X'pert score with the elimination of outliers, repeat compounds and insignificant scores. The candidate list shows the next highest X'pert score references that were not used for comparison. The reference patterns chosen against the sample in this case were Strontium Titanium Oxide (STO), Strontium Carbonate, and Titanium Oxide. As you can see in the Peak List each compound has several peaks in the diffraction spectra which match peaks in the spectrum of the sample. Excluding a repeat compound (SrCO<sub>3</sub>) all pattern list references scored 20 points higher on the X'pert score than the other candidates. In the final analysis of the X'pert software the program computes an estimate of the material composition of the sample. The Strontium Carbonate reference included in the pattern list did not have a RIR therefore quantifying phases of the sample exactly was impossible. The analysis can conclude that there was a reduction of Titanium Oxide and Strontium Carbonate and also there was an introduction of STO. The estimate composition is shown in the pie chart **Figure 4.4**

below; the color coding matches that of the peak list. The composition is estimated to be 36.6% Titanium Oxide, 59.4% Strontium Carbonate, and 4% Strontium Titanium Oxide (STO).

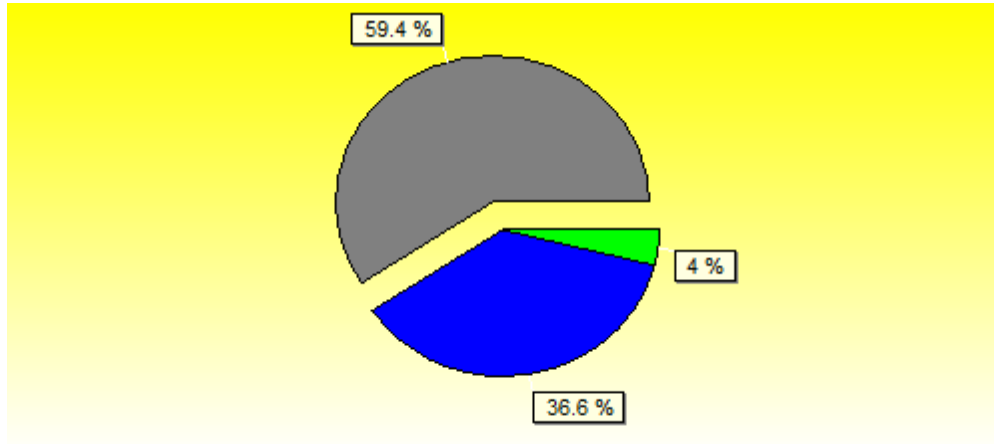


**Figure 4.4: Sample 1 Composition Estimate**

## 4.2 Sample 2 XRD Results

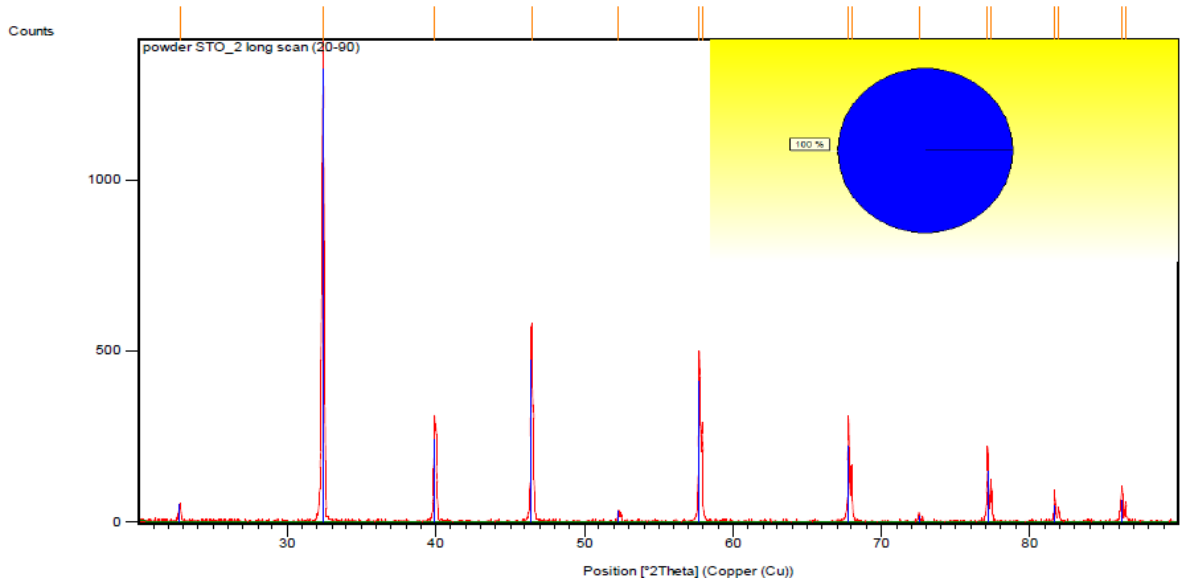


Figure 4.5: Sample 2 Diffraction Pattern

Figure 4.5 above is the spectral graph of the sample which was heated for twelve hours at thirteen hundred degrees Celsius. This graph gives the location and intensity peaks of the diffracted X-rays, which we can use to visually compare the sample to the reference data. Figure 4.6 shows few and very distinct peaks, this most likely means that interference from the diffraction pattern of one prevalent compound with possible trace elements is being represented. All diffraction peaks were identified in this sample.

### Peak List

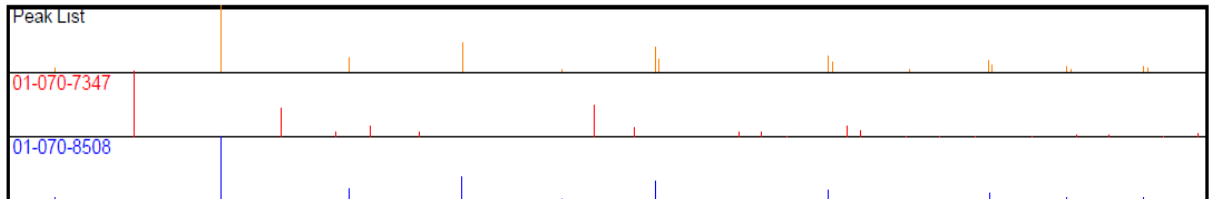


Figure 4.6: Sample 2 Peak List

### Pattern List

Ref.Code	Compound Name	Chem. Formula	Score	Scale Fac.
01-070-8508	strontium titanate	Sr ( Ti O3 )	94	0.949

### Candidate List

Ref.Code	Compound Name	Chem. Formula	Score	Scale Fac.
01-076-0741	tetrastrontium tri..	Sr4 Ti3 O10	17	0.051
00-022-1444	Strontium Titanium..	Sr4 Ti3 O10	16	0.040
01-080-1935	Strontium Titanium..	Sr Ti O2.60	15	0.145
00-047-0226	Strontium Titanium..	Sr Ti O2.72	9	0.180
01-089-3074	titanium suboxide	Ti O0.48	5	0.062
00-039-1471	Strontium Titanium..	Sr2 Ti O4	4	0.435
01-078-2479	tristrontium ditit..	Sr3 Ti2 O7	4	0.011

**Figure 4.7: Sample 2 Pattern and Candidate List**

**Figure 4.7** above shows the peak spectrum of first the sample and then the reference spectra that were chosen to compare against it. Diffraction patterns are labeled by their reference code which can be found in the pattern list. The pattern list shows which compounds were selected by the user to compare to the sample's diffraction pattern. References in the pattern list were selected from the candidate list based on highest X'pert score with the elimination of outliers, repeat compounds and insignificant scores. The candidate list shows the next highest X'pert score references that were not used for comparison. The reference pattern chosen against the sample in this case was only Strontium Titanium Oxide (STO), with an X'pert score 77 points higher than all other scores. As you can see in the Peak List, the Strontium Titanium Oxide reference diffraction peaks matches exactly with the diffraction peaks of the sample. In the final analysis of the X'pert software the program computes an estimate of the material composition of the sample which can be viewed as accurate because of the existence of complete RIR data in pattern list. This is shown in the pie chart **Figure 4.8** below; the color coding matches that of the peak list. The composition is estimated to be 99.9% Strontium Titanium Oxide (STO). The unidentified parts of the composition could be attributed to trace elements of higher order Strontium Titanium Oxide such as the first three compounds on the candidate list.

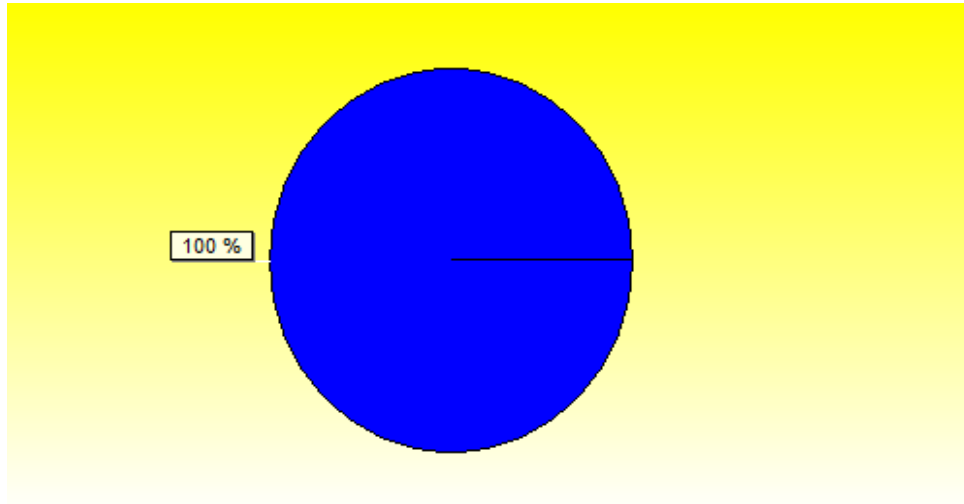


Figure 4.8: Sample 2 Composition Estimate

### 4.3 Sample 3 XRD Results

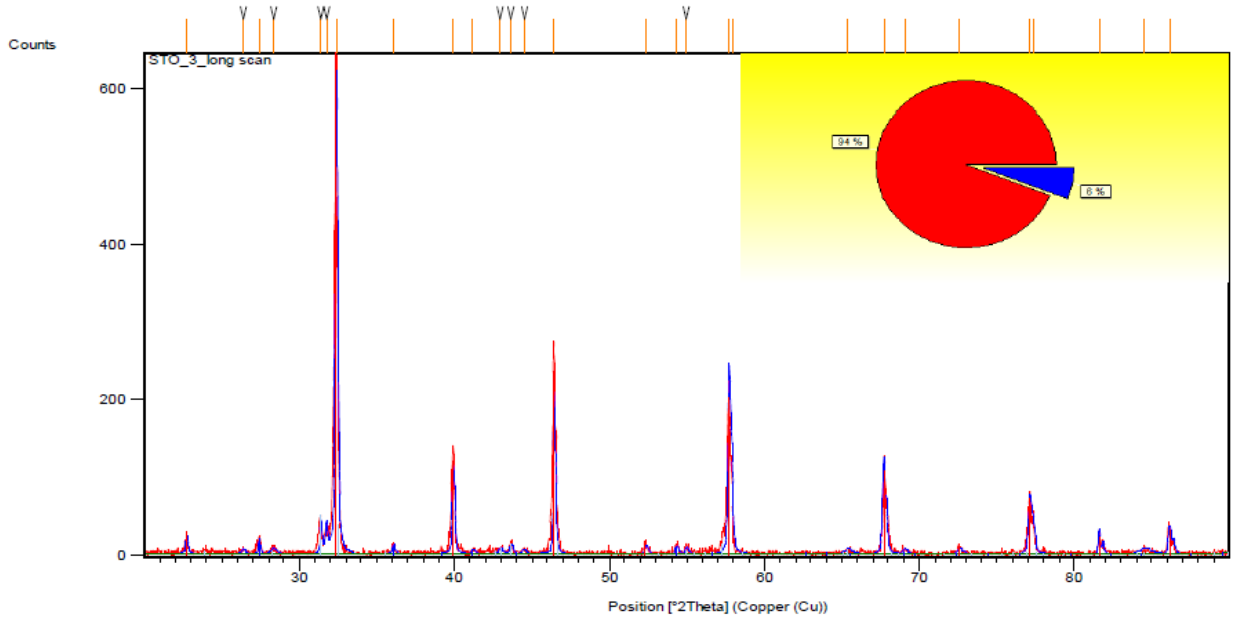


Figure 4.9: Sample 3 Diffraction Pattern

Figure 4.9 above is the spectral graph of the sample which was heated for ten hours at one thousand degrees Celsius. This graph gives the location and intensity peaks of the diffracted X-rays, which we can use to visually compare the sample to the reference data. Figure 4.10 shows few large peaks and several small peaks, this most likely means that interference from the diffraction pattern of several compounds is being represented. There are several unidentified small peaks which indicates trace element of an unidentified compound.

#### Peak List

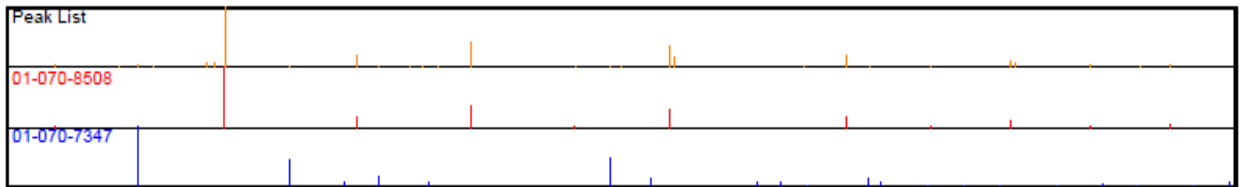


Figure 4.10: Sample 3 Peak List



### Pattern List

Ref.Code	Compound Name	Chem. Formula	Score	Scale Fac.
01-070-8508	strontium titanate	Sr ( Ti O3 )	76	1.010
01-070-7347	Rutile	Ti O2	32	0.031
01-071-2393	Strontianite	Sr C O3	Unmatch	0.529

### Candidate List

Ref.Code	Compound Name	Chem. Formula	Score	Scale Fac.
01-075-0444	Carbon	C	18	0.008
01-075-1621	Graphite-2H	C	17	0.008
00-041-1487	C.I. Pigment Black..	C	17	0.008
01-072-2040	á-( Sr O )2 Ti O2,..	( Sr O )2 Ti O2	14	0.074
00-039-1471	Strontium Titanium..	Sr2 Ti O4	13	0.080

**Figure 4.11: Sample 3 Pattern and Peak List**

**Figure 4.11** above shows the peak spectrum of first the sample and then the reference spectra that were chosen to compare against it. Diffraction patterns are labeled by their reference code which can be found in the pattern list. The pattern list showed which compounds were selected by the user to compare to the sample's diffraction pattern. References in the pattern list were selected from the candidate list based on highest X'pert score with the elimination of outliers, repeat compounds and insignificant scores. The candidate list shows the next highest X'pert score references that were not used for comparison. The reference patterns chosen against the sample in this case were Strontium Titanium Oxide (STO), Strontium Carbonate, and Titanium Oxide. As you can see in the Peak List each compound has several peaks in the diffraction spectra which match peaks in the spectrum of the sample. The pattern list references scored 14 points higher on the X'pert score than the other candidates with the exception of Strontium Carbonate. Strontium Carbonate was added to the pattern list because of its original existence in the powder.

In the final analysis of the X'pert software the program computes an estimate of the material composition of the sample. This is shown in the pie chart **Figure 4.12** below; the color coding matches that of the peak list. The composition estimated to be 6% Titanium Oxide, and 94% Strontium Titanium Oxide (STO).

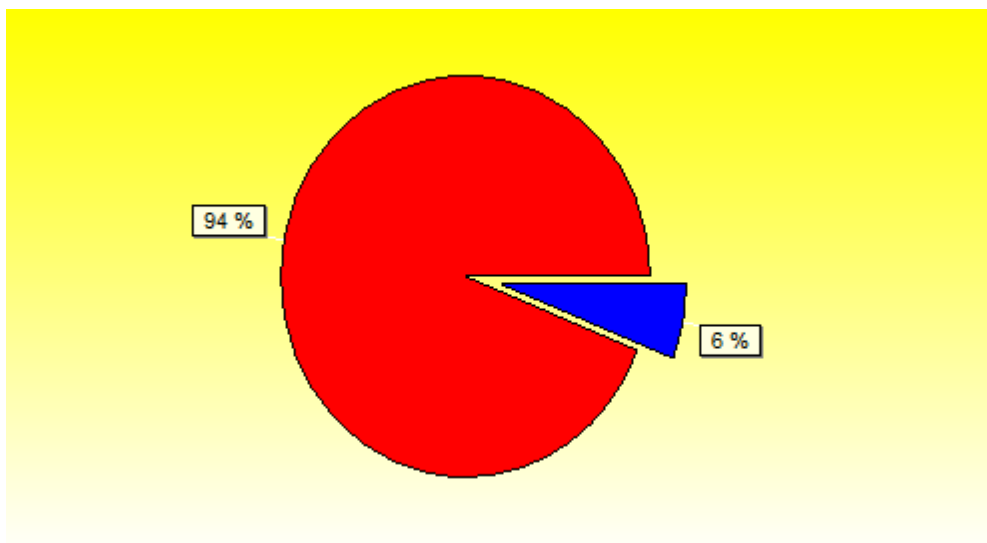


**Figure 4.12: Sample 3 Composition Estimate**

The unidentified peaks in this candidate list were found to be the result of a higher order Strontium Titanium Oxide compound, specifically  $\text{Sr}_2\text{TiO}_4$ . The inclusion of this reference in the pattern list eliminated the majority of the unidentified peaks. This compound was not included in the final data pattern list because it could be visually indicated to be a trace amount in the composition and because the RIR data was not included in the reference, therefore it would cause errors in the composition estimation.

## Dispersive X-ray Spectrometry

Only samples with high STO values shown in the XRD machine were selected to be analysis in the scanning electron microscope with dispersive X-ray spectrometry. These tools were used to measure powder shape and prove the existence of STO in the powder. Dispersive X-ray Spectrometry can identify elements and their concentrations in a sample, but it is unable to compare molecular compounds, unlike the XRPD.

### 4.4 Sample 2 EDX Results

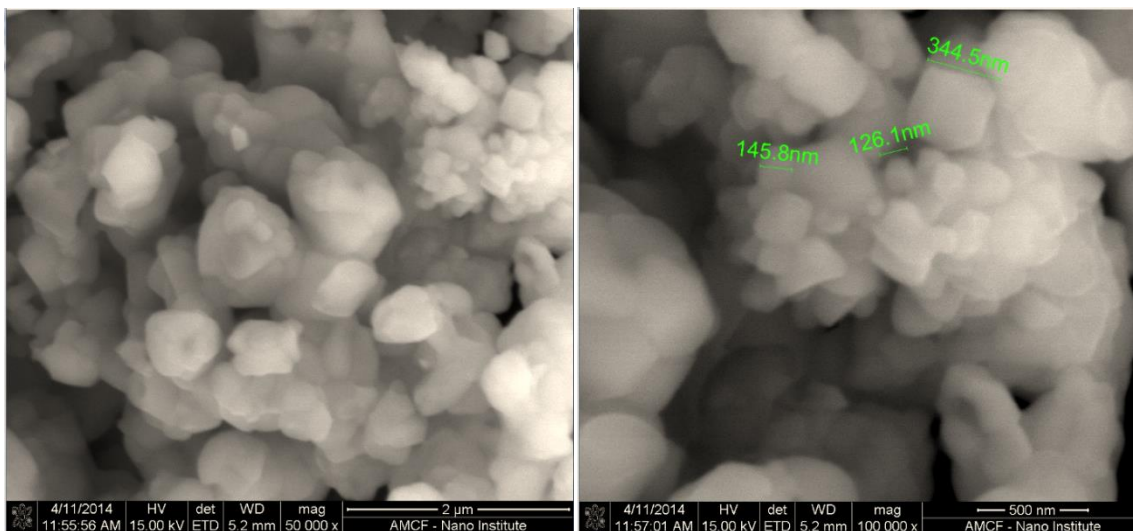


**Figure 4.13 and 4.14: SEM Photos**

Sample 2 was prepared according to the procedure then heated at 1300 degrees Celsius for 12 hours. The images shown in Figures **4.13-4.14** shown above are SEM images taken at two micrometers (**Figure 4.13**) and five hundred nanometers (**Figure 4.14**). These images show crystalline structure is the synthesized powder. The powder was not milled after the solid state process therefore larger conglomerates were possible. Crystals can be as small as 130 nanometers as shown in **Figure 4.14**.

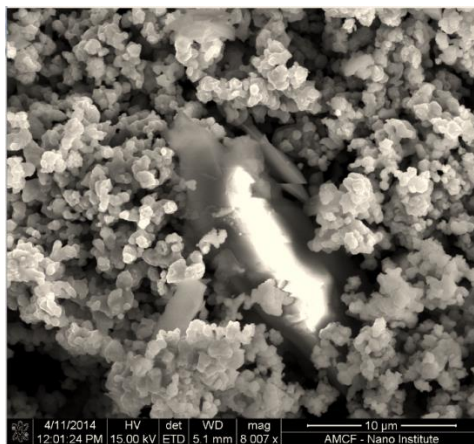


**Figure 4.15: SEM Contaminate Picture**

A Sodium contaminate was found in the sample, this was likely due to the handling of the sample and unavailability of vacuum storage after the solid state synthesis, the contaminate can be seen in **Figure 4.15**

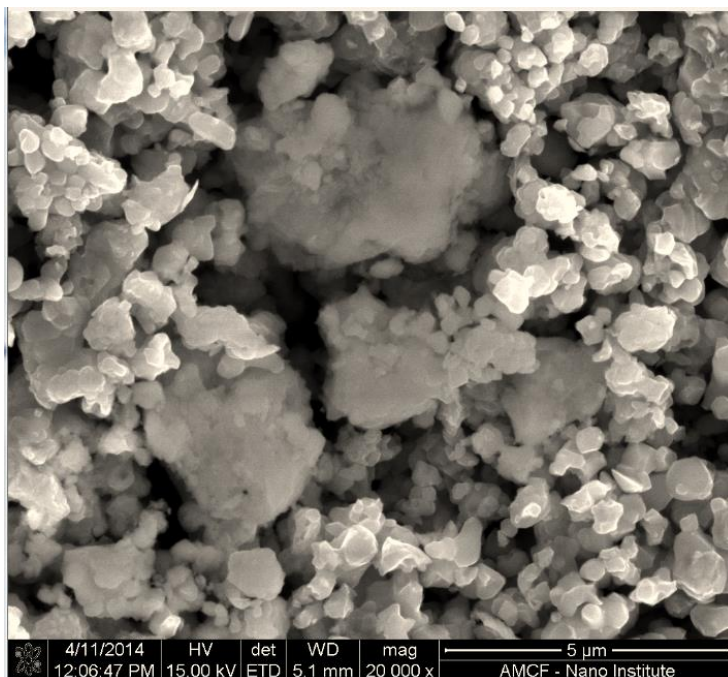


**Figure 4.16: SEM Conglomerates**

Large conglomerates of STO were found in later images, such as **Figure 4.16**. This phenomenon can be seen in the middle of the image. The formations are most likely due to nucleation of STO particles because of the twelve-hour heating time.

EDX scans were in complete agreement of the XRD results, showing SrTiO<sub>3</sub>, with only trace elements and impurities in the sample. Although the EDX cannot identify molecules it can approximate the amount of each element in a scanned area. Then the user can compare the atomic ratio in the area to that of the molecule. This was done for STO showing the accurate ratio, the data is shown below in **Figure 4.17**.

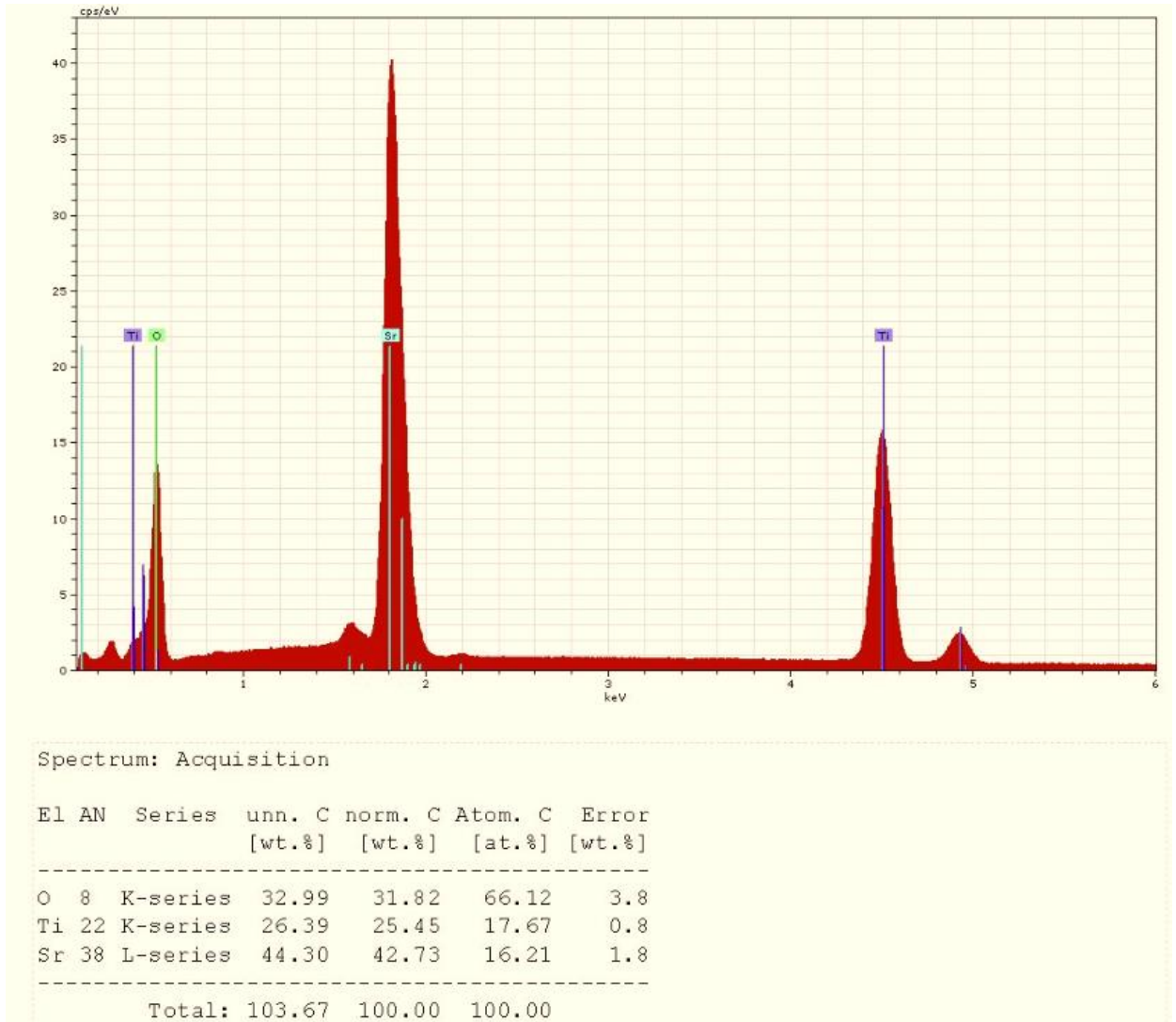


**Figure 4.17: Sample 2 EDX Data**

**Figure 4.17** shows intensity of X-ray's emitted verse the number of X-ray's recorded. The table shows the element, atomic number, un-normalized percentage weight, normalized percentage weight and percent of total atoms in the scanned area.

## 4.4 Sample 3 EDX Results

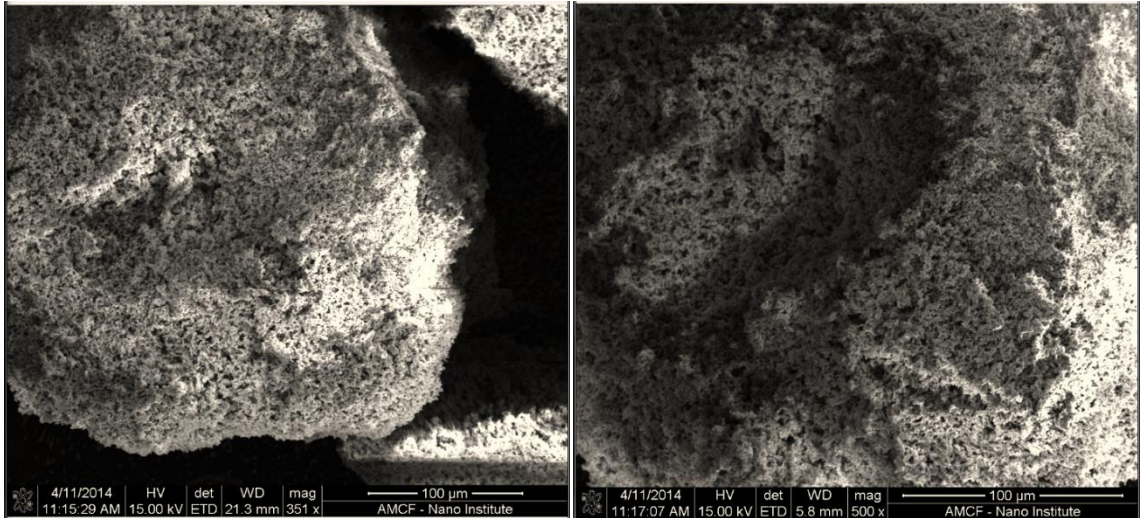


Figure 4.18 and 4.19: SEM Pictures

Sample 3 was prepared according to the procedure then heated at 1000 degrees Celsius for 10 hours. The images shown in **Figures 4.18-4.19** above are SEM images taken at one hundred micrometers. These images clearly show the powder kept its powder state throughout synthesis process. The powder was not milled after the solid state process therefore larger conglomerates are possible.

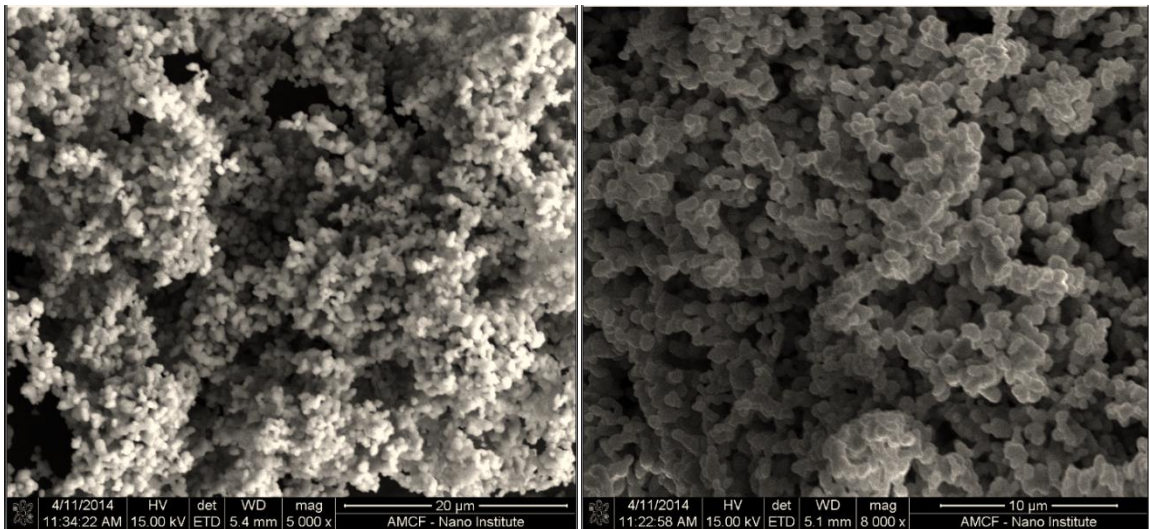


Figure 4.21 and 4.22: SEM Pictures

Large conglomerates of STO were not in sample 2. This could be attributed to the fact that the sample was heated for a shorter period of time or that the temperature of the sample never reached a temperature to initiate nucleation.

EDX scans were in complete agreement of the XRD results showing SrTiO<sub>3</sub>, with only trace elements and impurities in the sample. Although the EDX cannot identify molecules, it can approximate the amount of each element in a scanned area. Then the user can compare the atomic ratio in the area to that of the molecule. This was done for STO showing the accurate ratio, the data is shown below Figure 4.22.

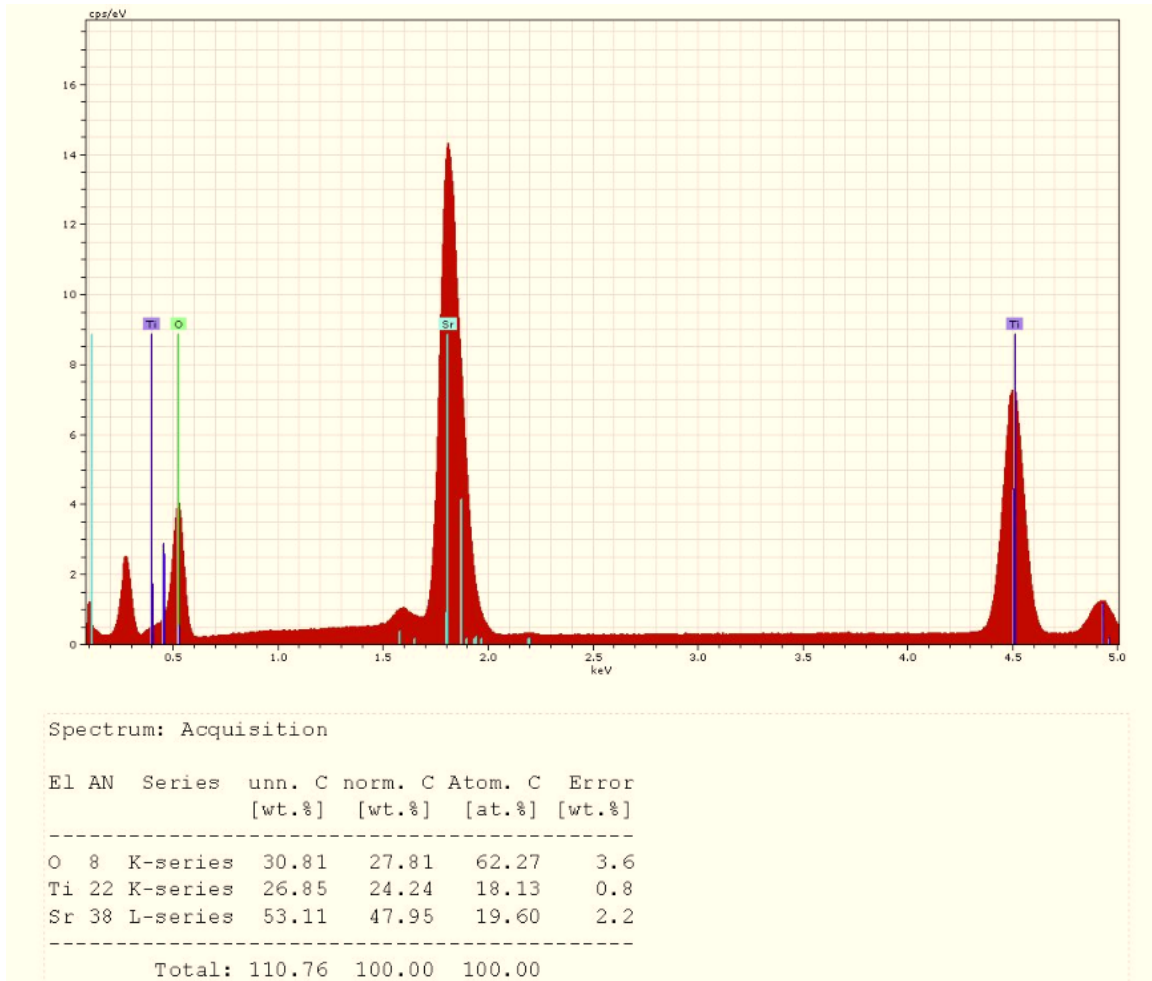
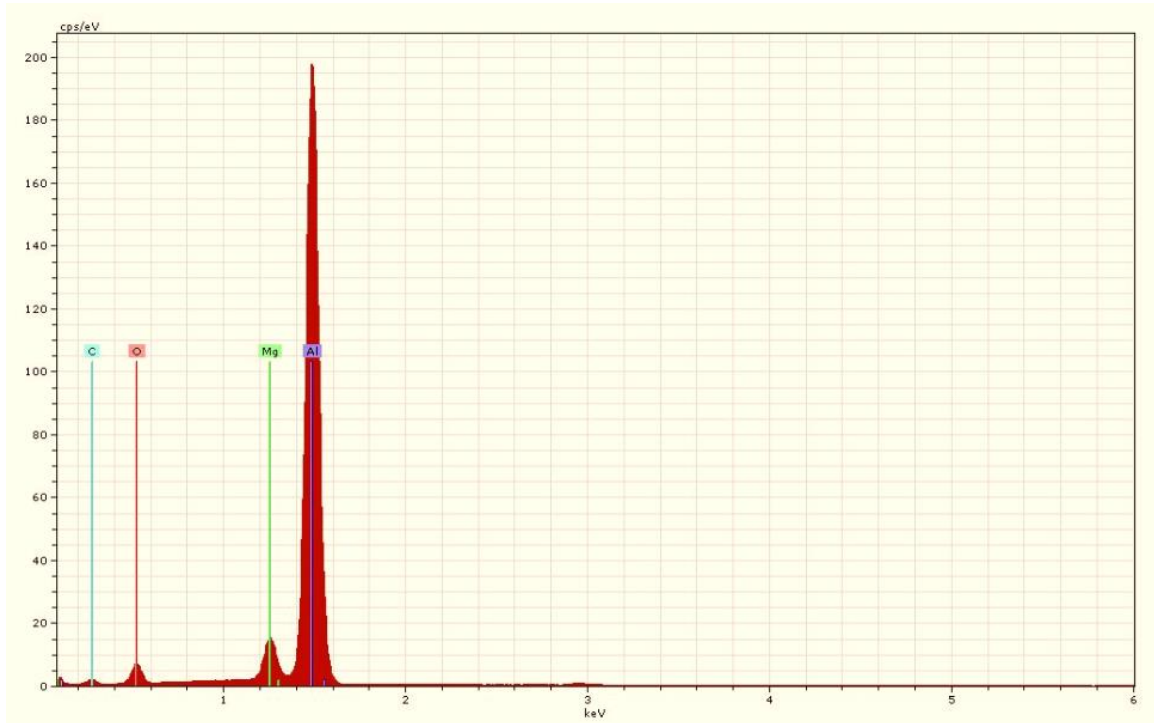


Figure 4.22: Sample 3 EDX Data

Both sample scans were showing small traces of magnesium contaminate in EDX scans. This was found to be caused by magnesium on the aluminum stud use to mount the sample in the microscope. The results of the EDX scan of the stud are shown below in **Figure 4.23**.



**Figure 4.23: Stud EDX Data**



## 5. Conclusions

XRPD results demonstrated that Strontium Titanium Oxide can be solid state synthesized from Strontium Carbonate and Titanium Oxide held at temperatures above 1300°C under optimal conditions for 10 hours following the discussed procedure. This data does not determine the size, or shape of Strontium Titanium Oxide but asserts the possibility of creation of Strontium Titanium Oxide with this procedure. An X'pert score of 92 points was recorded which was noted as the highest XRD purity score recorded in the University of Arkansas labs.

The EDX data is in complete agreement with XRD results, showing crystalline growth of STO nano-particles with sizes as small as 130 nanometers. SEM imaging results show the necessity of refining the original procedure to produce specific particle sizes to suit the needs of the user.

This could be as simple as mortaring after synthesis or changing temperature and heat times.

The solid state synthesis method was employed in this thesis for the economic value of producing less costly STO nano-particles. With this method producing one gram of STO powder has been reduced to the cost of \$5.33 per gram. Commercial grade 99.9% purity STO targets purchased by the University of Arkansas cost \$655.00 for the smallest available target. This target is approximate 12.2 grams in weight. With the solid state synthesis method a laboratory can produce 12.2 grams of STO for \$64.93 dollars, approximately one tenth of the price of commercial STO PLD targets, which are 12.2 grams in volume. At this rate the initial cost of the Carbolite furnace and materials cost will be recouped in the completion of fewer than sixteen STO targets. Therefore the solid state method for producing STO powders for the purpose of creating PLD targets is economically viable.

## 6. Future Work

This work demonstrates the practicality and ability for University of Arkansas labs to produce perovskite materials via solid state synthesis. Future work could be to optimize the solid state synthesis procedure for STO by varying temperature and heat time iterations. Other works describe high temperatures such as 1300 degrees Celsius only needing a heat time of one hour to produce 99.9% pure STO. [2] This could reduce production time and cost. Another candidate for solid state fabrication is  $\text{MgAl}_2\text{O}_4$ . It is a good insulating barrier to realize quantum confinement and a very good candidate for iso-structural growth of a spinel-type superlattice along the (111) orientation.

## Works Cited

- [1] L.F. da Silva, L.J.Q. Maiab, M.I.B. Bernardia, J.A. Andrésc and V.R. Mastelaroa, "An improved method for preparation of SrTiO<sub>3</sub> nanoparticles" *Materials Chem. and Phys.*, vol. 125, no. 1, pp. 168-173, Sept. 2010.
- [2] G.Viruthagiri\*, P.Praveen, S.Mugundan, and E.Gopinathan, "Synthesis and characterization of pure and nickel doped SrTiO<sub>3</sub> nanoparticles via Solid State Reaction Route" *Ind. Jour. of Adv. Chem. Scien.*, vol. 1, no. 3, pp. 132-138, Apr. 2013.
- [3] L.B. Freund and S. Suresh, "1.2.1 physcal vapor deposition" in *Thin Film Materials*, 2<sup>nd</sup> ed. United Kingdom, Cambridge , University Press., 2006, ch. 1 sec.1.2.1 pp. 6-9
- [4] R. Eason, "Pulsed laser deposition of complex materials: progress toward applications" in *Pulsed laser deposition of thin films*, 1<sup>st</sup> ed. Hoboken, New Jersey, John Wiley and Sons Inc., 2007, ch. 1 sec.1 pp. 3-28
- [5] D. Harevy. (1999) *Introduction to X-ray Diffraction (XRD)* (1<sup>st</sup> ed.) [Online] Available FTP: [http://www.asdlib.org/onlineArticles/ecourseware/Bullen\\_XRD/LearningActivity\\_Diffraction\\_BraggsLaw.pdf](http://www.asdlib.org/onlineArticles/ecourseware/Bullen_XRD/LearningActivity_Diffraction_BraggsLaw.pdf)
- [6] S. Swapp. (2013) *Scanning Electron Microscopy (SEM)* (1<sup>st</sup> ed.) [Online] Available FTP: [http://serc.carleton.edu/research\\_education/geochemsheets/techniques/SEM.html](http://serc.carleton.edu/research_education/geochemsheets/techniques/SEM.html)
- [7] Central Facility for Advanced Microscopy and Microanalysis University of California. (1996) *Introduction to Energy Dispersive X-ray Spectrometry (EDS)* (1<sup>st</sup> ed.) [Online] Available FTP: <http://micron.ucr.edu/public/manuals/EDS-intro.pdf>
- [8] H.P.R. Frederkise and W.R. Hosler, "Hall Mobility in SrTiO<sub>3</sub>" *Nat. Bureau Stand.*, vol. 161, no. 3, pp. 822-827, Nov. 1967.
- [9] A. F. Santander-Syro and O. Copie, "Two-dimensional electron gas with universal subbands at the surface of SrTiO<sub>3</sub>" *Moamlllan Pub. Lim.*, vol. 469, no. 1, pp. 189-194, Jan. 2011.

## Appendixes:

### A1 Oven Power Supply

A significant portion of the time and resources need for this work in went to the Installation and operation of the Carbolite oven used in the procedure. An obstacle to the project that took some time to overcome was the requirement of a new power source correct to run the oven. The Carbolite oven was designated as a RHF 16/3, 208V 1-phase, which requires a 40 amp power source (shown in the **Figure A1**).

Model	phases	Volts	Supply Fuse Rating
RHF 14/3	1-phase	200-240	32A (or 30A)
RHF 14/3	2-phase + N	380/220 - 415/240	16A/ph (or 15A)
RHF 15/3,16/3	1-phase	200-240	40A
RHF 15/3,16/3	2-phase + N	380/220 - 415/240	20A/ph
RHF 14/8	1-phase	200-240	63A
RHF 14/8	2-phase + N	380/220 - 415/240	32A/ph (or 30A)
RHF 15/8,16/8	1-phase	200-240	63A
RHF 15/8,16/8	3-phase + N	380/220 - 415/240	20A/ph
RHF 15/8,16/8	3-phase delta	220-240	32A/ph
RHF 15/8,16/8	3-phase delta	208	40A/ph
RHF 14/15	3-phase + N	380/220 - 415/240	25A
RHF 14/15	3-phase delta	220-240, 208	40A/ph
RHF 15/15,16/15	3-phase + N	380/220 - 415/240	25A/ph
RHF 15/15,16/15	3-phase delta	220-240, 208	50A/ph
RHF 15/15,16/15	3-phase + N	380/220 - 415/240	25A/ph
RHF 15/15,16/15	3-phase delta	220-240, 208	50A/ph
RHF 14/35, 15/35	3-phase + N	380/220 - 415/240	40A/ph
RHF 14/35, 15/35	3-phase delta	220-240, 208	63A/ph
RHF 16/35	3-phase + N	380/220 - 415/240	40A/ph ( <i>see note</i> )
RHF 16/35	3-phase delta	220-240, 208	63A/ph ( <i>see note</i> )

*380-415V 3-wire: same ratings as 3-phase+N*

**Figure A1:Power Source Chart**

After the correct power supply was installed the oven was moved in to the correct position.

### A1.2 Oven Setup

After positioning the oven, the four Silicon Carbide heating elements were slid in position into the oven and the chimney was attached. Then the oven was wired according to the 200-240V circuit 2 shown below in **Figure A2**.

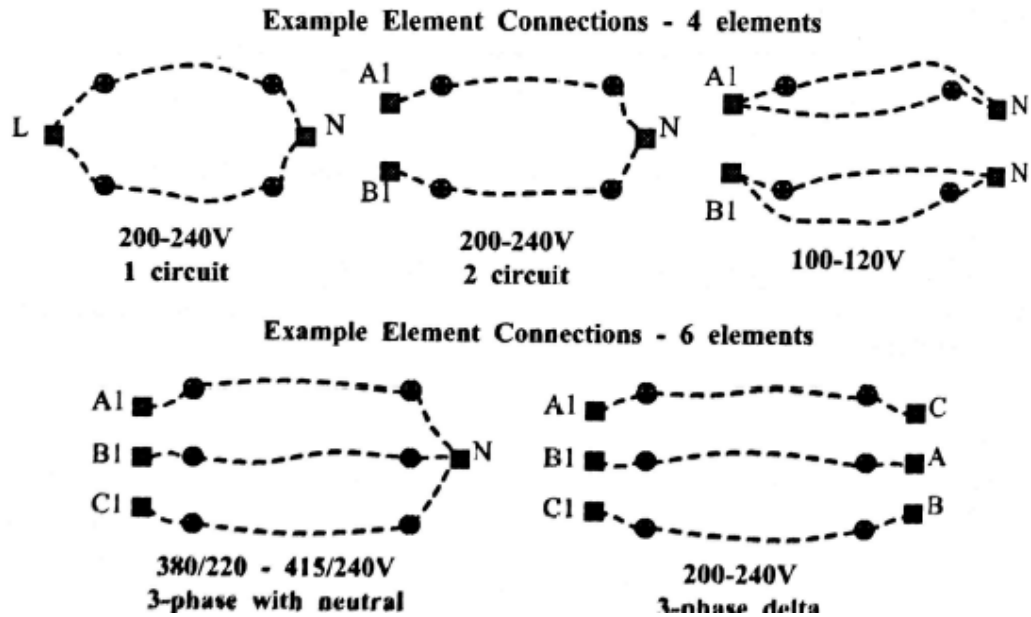


Figure A2: Wiring Chart

After the oven was correctly wired, the initial heating had to be conducted. The thermal insulating materials used in the construction of the Carbolite furnace contain organic binders. These binders are released during the first heating cycles. The furnace was heated to its maximum rated temperature, 1600 degrees C, and held there for an hour.

### A1.3 Oven Program Setup

The heating process as described in the procedure was controlled by a program run on the ovens internal computer. The program ran in three cycles, each controlled by three variables: the “rate per minute” (RPM), the increase in the temperature in degrees Celsius of the oven per minute; the “temperature set point”, the temperature at which the oven would begin to dwell; and the “dwell time” (DWEL), a set period of time in which the oven would hold the set point temperature before starting the next cycle. It is important to note the after the final programmed dwell time the oven will stop supplying heat. The programs for each specific sample are shown below in **Figure A3**.

Cycle	Step	Sample 1	Sample 2	Sample 3
1	RMP	5.0 C/min	5.0 C/min	5.0 C/min
1	TSP	600 C	600 C	600 C
1	DWEL	15 min	15 min	15 min
2	RMP	5.0 C/min	5.0 C/min	5.0 C/min
2	TSP	800 C	1300 C	1000 C
2	DWEL	8 hrs	12 hrs	10 hrs
3	RMP	5.0 C/min	5.0 C/min	5.0 C/min
3	TSP	600 C	600 C	600 C
3	DWEL	15 min	15 min	15 min

Figure A3: Sample Programs

### B1 Reference Data Peak lists

The Figure B1 below is the peak list for the SrTiO<sub>3</sub> reference used in the analysis of the sample.

### Peak list

No.	h	k	l	d [Å]	2Theta[deg]	I [%]
1	1	0	0	3.90000	22.783	12.0
2	1	1	0	2.75900	32.424	100.0
3	1	1	1	2.25300	39.985	30.0
4	2	0	0	1.95200	46.485	50.0
5	2	1	0	1.74600	52.358	3.0
6	2	1	1	1.59400	57.796	40.0
7	2	2	0	1.38100	67.805	25.0
8	3	0	0	1.30200	72.545	1.0
9	3	1	0	1.23500	77.177	15.0
10	3	1	1	1.17740	81.724	5.0
11	2	2	2	1.12730	86.206	8.0
12	3	2	1	1.04370	95.131	16.0
13	4	0	0	0.97650	104.154	3.0
14	4	1	1	0.92050	113.613	10.0
15	3	3	1	0.89590	118.590	3.0
16	4	2	0	0.87310	123.832	10.0
17	3	3	2	0.83250	135.423	6.0
18	4	2	2	0.79720	150.147	9.0

Figure B1: STO Reference Peak List

The **Figure B2** below is the peak list for the TiO<sub>2</sub> reference used in the analysis of the sample.

### **Peak list**

No.	h	k	l	d [Å]	2Theta[deg]	I [%]
1	1	1	0	3.24700	27.447	100.0
2	1	0	1	2.48700	36.086	50.0
3	2	0	0	2.29700	39.188	8.0
4	1	1	1	2.18800	41.226	25.0
5	2	1	0	2.05400	44.052	10.0
6	2	1	1	1.68740	54.323	60.0
7	2	2	0	1.62370	56.642	20.0
8	0	0	2	1.47970	62.742	10.0
9	3	1	0	1.45280	64.040	10.0
10	2	2	1	1.42430	65.480	2.0
11	3	0	1	1.35980	69.010	20.0
12	1	1	2	1.34650	69.790	12.0
13	3	1	1	1.30410	72.410	2.0
14	3	2	0	1.27390	74.411	1.0
15	2	0	2	1.24410	76.510	4.0
16	2	1	2	1.20060	79.822	2.0
17	3	2	1	1.17020	82.335	6.0
18	4	0	0	1.14830	84.260	4.0
19	4	1	0	1.11430	87.464	2.0
20	2	2	2	1.09360	89.557	8.0
21	3	3	0	1.08270	90.708	4.0
22	4	1	1	1.04250	95.275	6.0
23	3	1	2	1.03640	96.017	6.0
24	4	2	0	1.02710	97.177	4.0
25	3	3	1	1.01670	98.514	1.0
26	4	2	1	0.97030	105.099	2.0
27	1	0	3	0.96440	106.019	2.0
28	1	1	3	0.94380	109.406	2.0
29	4	0	2	0.90720	116.227	4.0
30	5	1	0	0.90090	117.527	4.0
31	2	1	3	0.88920	120.059	8.0
32	4	3	1	0.87740	122.788	8.0
33	3	3	2	0.87380	123.660	8.0
34	4	2	2	0.84370	131.847	6.0
35	3	0	3	0.82920	136.549	8.0
36	5	2	1	0.81960	140.052	12.0
37	4	4	0	0.81200	143.116	2.0
38	5	3	0	0.78770	155.870	2.0

**Figure B2: TiO<sub>2</sub> Reference Peak List**

The **Figure B3** below is the peak list for the SrCO<sub>3</sub> reference used in the analysis of the sample.

### **Peak list**

No.	h	k	l	d [Å]	2Theta[deg]	I [%]
1	1	1	0	4.36700	20.319	14.0
2	0	2	0	4.20700	21.101	6.0
3	1	1	1	3.53500	25.172	100.0
4	0	2	1	3.45000	25.803	70.0
5	0	0	2	3.01400	29.615	22.0
6	1	2	1	2.85900	31.261	5.0
7	0	1	2	2.83800	31.498	20.0
8	1	0	2	2.59600	34.522	12.0
9	2	0	0	2.55400	35.108	23.0
10	1	1	2	2.48100	36.176	34.0
11	1	3	0	2.45800	36.527	40.0
12	0	2	2	2.45110	36.633	33.0
13	2	1	1	2.26460	39.772	5.0
14	2	2	0	2.18310	41.323	16.0
15	0	4	0	2.10350	42.963	7.0
16	2	2	1	2.05260	44.083	50.0
17	0	4	1	1.98600	45.643	26.0
18	2	0	2	1.94890	46.563	21.0
19	1	3	2	1.90530	47.694	35.0
20	1	4	1	1.85140	49.173	3.0
21	1	1	3	1.82530	49.923	31.0
22	0	2	3	1.81340	50.274	16.0
23	2	3	1	1.80230	50.605	4.0
24	2	2	2	1.76850	51.643	7.0
25	0	4	2	1.72530	53.035	5.0
26	3	1	0	1.66840	54.994	3.0
27	2	4	0	1.62360	56.646	4.0
28	3	1	1	1.60800	57.246	13.0
29	1	5	0	1.59810	57.634	3.0
30	2	4	1	1.56760	58.864	13.0
31	1	5	1	1.54470	59.824	11.0
32	0	0	4	1.50720	61.472	3.0
33	2	2	3	1.47820	62.813	6.0
34	3	1	2	1.45960	63.707	4.0
35	3	3	0	1.45510	63.927	9.0
36	2	4	2	1.42930	65.222	6.0
37	1	1	4	1.42460	65.464	7.0
38	1	5	2	1.41200	66.123	5.0
39	0	6	0	1.40240	66.634	4.0
40	3	3	2	1.31030	72.014	10.0
41	2	0	4	1.29770	72.824	4.0
42	3	1	3	1.28400	73.729	13.0
43	4	0	0	1.27660	74.228	4.0

**Figure B3: SrCO<sub>3</sub> Reference Peak List**